Journal of Materials Chemistry A

Accepted Manuscript

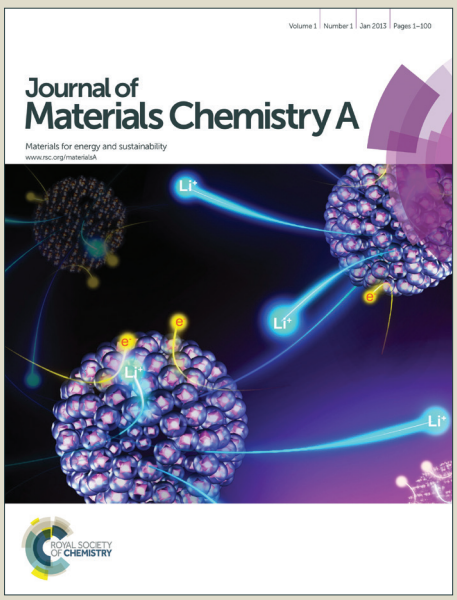

ROYAL SOCIETY OF CHEMISTRY

www.rsc.org/materialsA

Journal of Materials Chemistry A

Journal of Materials Chemistry A

Dynamic Article Links ►

Cite this: DOI: 10.1039/c0xx00000x

ARTICLE TYPE

www.rsc.org/xxxxxx

Design of the enzymatic biofuel cell with large power output†

Yun Chen,[‡a] Panpan Gai,[‡a] Jianrong Zhang,*[a, b] and Jun-Jie Zhu*[a]

Received (in XXX, XXX) Xth XXXXXXXXX 20XX, Accepted Xth XXXXXXXXX 20XX
DOI: 10.1039/b000000x

Enzymatic biofuel cell (EBFC), utilizing redox enzymes as the catalysts to produce energy from green and renewable fuels, is considered as the promising environmental-friendly power source. However, EBFC is mainly limited by the electron transfer barrier between enzymes and electrodes, which is the major rate-limiting step to hinder the improvement of EBFC power output. In this study, enzymes were effectively bound to the hydrophilic and carboxyl group functionalized graphene–gold nanoparticle hybrid, and the hybrid as electrode material could also speed up the electron transfer in the EBFC. The open circuit voltage (E_{cell}^{ocv}) of the designed EBFC could reach to 1.16 ± 0.02 V, and the maximal power density (P_{max}) was as high as 1.96 ± 0.13 mW cm^{-2}. Based on both the as-prepared EBFC units in series, the red and yellow light-emitting diodes (LEDs) were successfully lighted, respectively, and the E_{cell}^{ocv} and P_{max} could keep 80% and 66% of the optimal value over 70 days, respectively. The fabricated EBFC is expected to be applied in the bioenergy fields.

1. Introduction

In order to overcome the ever-increasing crisis of the traditional non-renewable energy consumption, researchers have tried to find some efficient methods for converting chemical energy into electrical energy.[1] Biofuel cells (BFCs), involving the use of enzymes (enzymatic biofuel cells, EBFCs) or microorganisms as catalysts, are able to oxidize targeted biofuel and reduce oxidizer at specific electrodes to harvest energy.[1-4] Compared to the traditional fuel cells, BFCs have some special advantages. Firstly, unlike the noble metals catalysts with the expensive charge and the limited storage, biological catalysts have the plentiful and reproducible sources. Secondly, in BFCs, the renewable biofuels from plants and animals are used as fuels at the anode, while O_2 usually serves as oxidizer at the cathode. Because the products of the reaction in BFCs are non-toxic,[5] BFCs are biocompatible and can be minimized as an implantable power supply for medical devices,[3, 6-8] Finally, most of the BFCs can generate electricity under mild conditions. As a result, it is foreseen that BFC is one of the next-generation green and potential sustainable energy devices.

Although BFC represents a new power source, it is still difficult for its commercial applications. In contrast to the traditional fuel cells, the applicability of BFCs is limited by several factors, including the low open circuit voltage (E_{cell}^{ocv}), insufficient power output, and long-term instability.[1, 2] Generally, in the case of EBFCs, glucose oxidase (GOD) is used for catalyzing the oxidation of glucose at the anode, and laccase is applied to the reduction of O_2 at the cathode, therefore, the electrical contacting of redox enzymes with electrodes is of fundamental significance for the development of EBFCs.[9] Because the active centres of most redox enzymes are deeply buried within the protein matrices, it is difficult for direct electron transfer (DET) between the enzymes and the electrodes.[1-3] The poor electron transfer results in the low power densities of EBFCs. At present, the maximal E_{cell}^{ocv} for a single EBFC unit has reported to be 0.95 V.[10, 11] The maximal power density (P_{max}) reached to 1.45 ± 0.24 mW cm^{-2},[12] and the active lifetimes were typically 8 hours to 30 days.[1, 10]

The nanoparticles with the high electrochemical stability and good conductivity can be selected as ideal conducting channels to promote efficient DET between enzyme and electrodes.[4] Recently, we fabricated the hydrophilic and carboxyl group functionalized graphene–gold nanoparticles (AuNPs) hybrid for glucose electrochemical biosensing[13] and demonstrated the hybrid could provide a suitable microenvironment for GOD to retain its biological activity. The DET between GOD and the hybrid electrode could be realized without electron mediator.

Herein, the graphene–AuNPs hybrid electrode was used for designing EBFC, as shown in Scheme 1. The morphology of the graphene–AuNPs hybrid is shown in Fig. S1 in the ESI. In the bioanode compartment, GOD could bind to the graphene–AuNPs hybrid,[13] and glucose was oxidized to gluconolactone without redox mediator under anaerobic conditions; gluconolactone was further oxidized to gluconic acid by the role of the graphene–AuNPs hybrid. The electrons produced in the bioanode compartment flowed through an external circuit load to the biocathode compartment, where O_2 was reduced to H_2O. The biocathode was composed of laccase bound to the graphene–AuNPs hybrid as biocatalyzer, and 2,2'-azinobis (3-ethylbenzthiazoline-6-sulfonic acid) diammonium salt (ABTS) as

a redox mediator (saturated with O_2). Because laccase is often inactive at neutral pH, and usually requires an environment of pH 5.0,[5, 14] the acetic acid buffer solution was selected as electrolyte. The two compartments were separated with nafion membrane. In the EBFC, the E_{cell}^{ocv} and the P_{max} could reach to 1.16 ± 0.02 V and 1.96 ± 0.13 mW cm^{-2}, respectively, and E_{cell}^{ocv} and P_{max} could still keep 80% and 66% of the optimal value after 70 days, respectively. The red and yellow light-emitting diodes (LEDs) could be successfully lighted by the two as-fabricated EBFC unit in series.

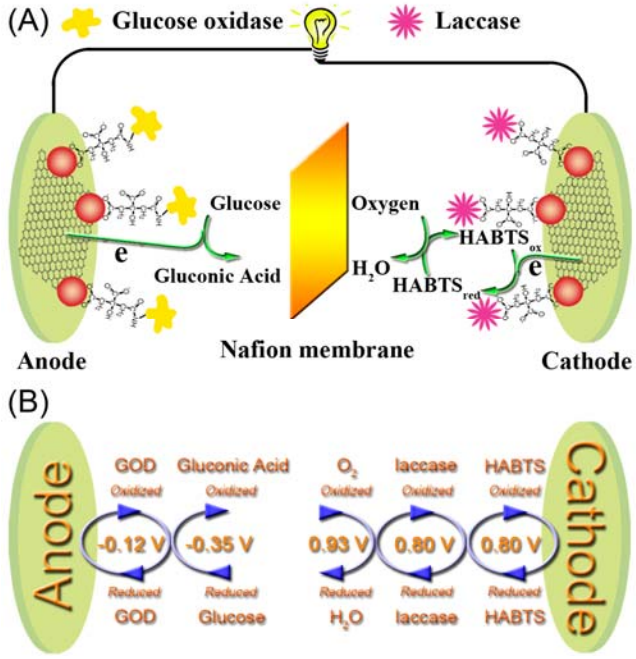

Scheme 1. (A) Principle of operation of the EBFC based on the graphene–AuNPs hybrid anode and cathode, and (B) the formal redox potentials (*vs.* SHE, pH = 5.0) schematic for the EBFC.

2. Experimental

2.1 Chemicals.

The hydrophilic and carboxyl group functionalized graphene–AuNPs hybrid, which was suitable for the binding of enzymes stably by the condensation reaction with amino group, was fabricated by our previous work.[13] GOD from *Aspergillus niger* (EC 1.1.3.4, 294 units mg^{-1}) was purchased from Sanland. Laccase from *Trametes versicolor* (EC 1.10.3.2, > 20 units mg^{-1}) and 2,2'-azinobis (3-ethylbenzothiazoline-6-sulfonic acid) diammonium salt (ABTS) were from Sigma-Aldrich. Both of the enzymes were used as received without further purification. Glucose was obtained from Sinopharm, and the glucose stock solution (1 M) was prepared at least 24 h before use. 0.2 M acetic acid buffer solution (pH 5.0) was made from acetic acid and sodium acetate anhydrous. Aqueous solutions were prepared with ultrapure water from an Elix 5 Pure Water System (> 18 MΩ cm).

2.2 Instrumentation.

The morphology of the graphene–AuNPs hybrid was characterized by a field emission scanning electron microscopy (FESEM, HITACHI S4800). Electrochemical measurements were performed using a workstation (CHI 660B). Cyclic voltammetric measurements were performed with a traditional three-electrode system including a Pt wire electrode as the counter electrode, a saturated calomel electrode (SCE) as the reference electrode, and the modified Au substrate as the working electrode. The open circuit potentials of the electrodes were tested with a two-electrode configuration (SCE as the reference electrode).

2.3 Preparation of bioanode and biocathode.

The Au substrates (1 cm × 0.5 cm) were provided by the 55th Institute of China Electronic Group (Nanjing, China). The Au substrates were prepared by sputtering 200 nm Au onto the quartz wafers with a few nanometers of Cr adhesion layer in vacuum.[15] Before using, the Au substrates were carefully scraped to a mirror finish by pledget, then, they were rinsed and sonicated by ethanol and ultrapure water, respectively, and dried under nitrogen flow.

The bioanode of the EBFC was fabricated referring to the reference.[13] Under the optimal conditions, 240 μg cm^{-2} graphene–AuNPs hybrid was dropped onto the Au substrate, and then the electrode was left to dry in an oven desiccator and stored at 37 °C. Then, the graphene–AuNPs hybrid electrode was immersed in a solution containing 1 mg mL^{-1} 1-ethyl-3-(3-dimethyl-aminopropyl) carbodiimide hydrochloride (EDC) and *N*-hydroxysuccinimide (NHS) for 3 h. After rinsing with ultrapure water to get rid of the excess EDC and NHS, the activated electrodes were immersed in 1 mL of GOD solution (10 mg mL^{-1}, dissolved in 0.05 M pH 9.0 tris-HCl solution) at 4 °C for 24 h. The biocathode of the EBFC was prepared as follows, after the fabrication of the graphene–AuNPs hybrid electrode, 50 μL of the laccase solution (60 mg mL^{-1}, dissolved in 0.05 M pH 7.0 PBS solution) was dropped to the graphene–AuNPs hybrid electrode and stored at 4 °C. Before the assembly of the EBFC, both of the prepared graphene–AuNPs–GOD hybrid electrode and the graphene–AuNPs–laccase hybrid electrode were purged with ultrapure water to wipe off unbound enzymes, and the electrodes were stored at 4 °C when they were not in use.

2.4 Biofuel cell design.

The perfluorosulfonic acid/PTFE copolymer membrane (DuPont™ Nafion® PFSA NRE-211), with thickness 25.4 μm, was used to separate the anodic and cathodic compartments. The anolyte was 0.2 M acetic acid buffer solution (pH 5.0) containing 50 mM of glucose saturated with nitrogen. The oxygen-saturated 0.2 M acetic acid buffer solution (pH 5.0) performed as the catholyte containing 0.5 mM of ABTS. The EBFC was performed at room temperature (25 °C). After a stable E_{cell}^{ocv} was observed, the variable external load ranged from 100 Ω to 100 kΩ was connected in series between anode and cathode. Then the power outputs were obtained with a precision digital multimeter.

3. Results and discussion

3.1 The characters of the bioanode.

In the bioanode, glucose oxidase first catalyzes the oxidation of β-D-glucose into D-glucono-1,5-lactone as follows: glucose → gluconolactone + 2H$^+$ + 2e (φ' = −0.24 V *vs.* SHE at pH 5.0). However, D-glucono-1,5-lactone can hydrolyze to gluconic acid further, but the process of hydrolysis is not fast enough.

According to Claus's report,[16] gold nanoparticles–carbon materials is the preferred catalyst for the oxidation of functional groups (-OH, C=O). Therefore, the gold nanoparticle–graphene hybrid in the bioanode can deeply oxidize glucose to gluconic acid, and the reaction at the bioanode should be as follows,

$$\text{glucose} \xrightarrow{\text{GOD, graphene-AuNPs}} \text{gluconic acid} + 2H^+ + 2e \quad E_a^{o'} = -0.35 \text{ V (}vs\text{. SHE)} \quad (1)$$

where $E_a^{o'}$ is the formal potential at pH 5.0, and the potential of –0.35 V (*vs*. SHE) is calculated by Nernst equation according to the formal potential of gluconic acid/glucose couple ($E_a^{o'}$ = –0.45 V *vs*. SHE) at pH 7.0.[17] Under the open circuit potential (OCP) condition, when SCE was used as the reference electrode (E_{ref} = 0.24 V), E_a^{ocp} was calculated to be –0.59 V. The measurement of the E_a^{ocp} was performed in 0.2 M acetic acid buffer solution (pH 5.0) which was saturated with N_2. E_a^{ocp} was recorded immediately after the circuit was closed, and the result was shown in Fig. 1A. It showed that the onset of E_a^{ocp} was –0.36 V (or –0.12 V *vs*. SHE), which was equal to the formal potential of GOD ($E_{GOD}^{o'}$) as shown in Scheme 1B. Curve b in Fig. 1A demonstrated that the E_a^{ocp} rapidly retained at –0.58 ± 0.01 V (n=3) (or –0.34 V *vs*. SHE), approaching to the speculated value, when there was 50 mM glucose in the testing solution. While curve a in Fig. 1A displayed that the E_a^{ocp} only reached to 0.062 ± 0.012 V (n=3) when there was no glucose in the testing solution. The E_a^{ocp} result demonstrated that the OCP of the bioanode was eventually determined by the thermodynamic potentials of the fuel, gluconic acid/glucose couple.[18, 19]

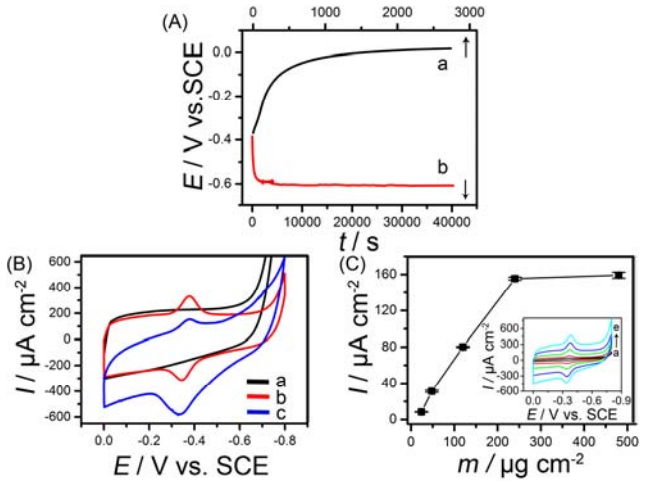

Fig. 1 (A) OCP of the graphene–AuNPs–GOD hybrid electrode in pH 5.0 electrolyte solution (a) without glucose and (b) with 50 mM glucose. (B) CVs of (a) graphene–AuNPs hybrid electrode, (b) graphene–AuNPs–GOD hybrid electrode only in pH 5.0 buffer solution and (c) graphene–AuNPs–GOD hybrid electrode in pH 5.0 electrolyte solution containing 1 mM glucose. (C) The relationship between the reduction peak currents of the bound GOD and the amount of the graphene–AuNPs hybrid only in pH 5.0 buffer solution. Every point was an average value of three independent measurements. Inset: CVs of graphene–AuNPs–GOD hybrid electrodes modified by various masses of the graphene–AuNPs hybrid: (a) 24 μg cm^{-2}, (b) 48 μg cm^{-2}, (c) 120 μg cm^{-2}, (d) 240 μg cm^{-2}, and (e) 480 μg cm^{-2}. The scan rate of (B) and (C) was 10 mV s^{-1}. All solutions were saturated with N_2.

The current density (i) in the bioanode influences on the power output of the EBFC, which can be expressed as follows:

$$i = nFk^0 \left[\Gamma_O(0,t) e^{-\alpha f(E-E^{0'})} - \Gamma_R(0,t) e^{(1-\alpha) f(E-E^{0'})} \right] \quad (2)$$

where the meaning of all the symbols is the same as the reference.[20] According to the equation (2), i relies on the electron transfer rate constant (k^0) that is affected by the electrode materials. In our former measurement for the graphene–AuNPs–GOD hybrid with glass carbon substrate electrode, k^0, the rate of the direct electron transfer of GOD, was evaluated as 7.74 ± 0.16 s^{-1}.[13] For comparison, Au was selected as the substrate electrode in the fabrication of bioanode. Cyclic voltammograms (CVs) of graphene–AuNPs hybrid modified Au electrode (curve a) and graphene–AuNPs–GOD hybrid modified Au electrode (curve b) were shown in Fig. 1B, and Fig. S2 in the ESI also showed CVs of the AuNPs, graphene, AuNPs–GOD, and graphene–GOD modified Au electrode, respectively. In contrast to curve a in Fig. 1B, curve b in Fig. 1B shows a couple of well-defined redox peaks at –0.38 and –0.35 V, respectively, which can be ascribed to the characteristic peaks of GOD (also see Fig. S3 in the ESI).[21] The peak-to-peak separation and the formal potential for GOD were obtained accordingly, which are 29 mV and –0.36 V (or –0.12 V *vs*. SHE), respectively, and k^0 was calculated to be 12.50 ± 0.27 s^{-1}. Compared to curve b in Fig. 1B, curve c showed that the oxidative peak increased while the reductive peak decreased when 1 mM glucose was added into the testing solution, which demonstrated that graphene–AuNPs–GOD could bioelectrocatalyze the oxidation of glucose directly in an E_rC_i-type catalytic reaction.[20] However, for graphene electrode and AuNPs electrode, when glucose was added into the testing solution, there was nearly no change comparing to the CVs results of these electrodes in the same solution without glucose, respectively. The results supported that the electron transfer from glucose to electrode *via* GOD was extremely fast, and Au was also the more suitable substrate material for the bioanode modified with the graphene–AuNPs–GOD hybrid.

However, at carbon nanotube (CNT) electrode, Stevenson's group[22] and Gorski's group[23] observed no changes for the redox peaks of GOD when the CNT–GOD electrodes were placed in the O_2-free testing solution with glucose, and concluded no DET between catalytic center of GOD and CNT electrode. It has been reported that functional nanomaterials could provide an electron-mediating function to facilitate the DET of enzymes by reducing the electron tunnelling distance between their active sites and electrode, therefore, there are already several papers reporting the detection of glucose based on the DET of glucose oxidase, such as by electrochemically entrapping GOD in the inner wall of the highly ordered conductive polyaniline nanotubes;[24] covalently cross-linking GOD to boron-doped diamond electrode;[25] and incorporating GOD into the reduced graphene oxide–multiwalled carbon nanotubes dispersion.[26] The results in these literatures confirmed the bioelectrocatalytic activity of the electrical contacted GOD in the N_2-saturated testing solutions with the addition of glucose. In our design, AuNPs were attached to the surface of GOD near the flavin adenine dinucleotide (FAD) centre, and the electron transfer distance between the catalytic centre and electrode should be decreased, which facilitated the DET of enzymes.[27]

The current density of the bioanode, i, also depends on the

concentration of GOD (Γ_{GOD}) covered on bioanode. Γ_{GOD} was mainly affected by the amount of the graphene–AuNPs hybrid covered on the Au substrate, which controlled the binding of GOD. In order to estimate the optimal Γ_{GOD}, a series of bioanodes with various amount of the graphene–AuNPs–GOD were fabricated. Fig. 1C showed the relationship between the reduction currents of the bound GOD and the amount of the graphene–AuNPs hybrid. With an increase of the loading amount of the graphene–AuNPs hybrid from 24 μg cm^{-2} to 240 μg cm^{-2}, the reduction currents produced by the bound GOD enhanced linearly. Finally, the reduction current could reach to the maximal value of 155 μA cm^{-2}, and it kept almost unchanged when the amount of the graphene–AuNPs hybrid covered on Au substrate was more than 240 μg cm^{-2}. Also, the different concentrations of GOD for the fabrication of bioanode were tested, and the results were shown in Fig. S4 in the ESI, and it demonstrated that 10 mg mL^{-1} was the optimal concentration for GOD.

3.2 The characters of the biocathode.

For the reason above mentioned, Au substrate was also chosen as biocathode material. In the biocathode compartment, the oxygen was reduced to water at the biocathode as follows,

$$O_2 + 4H^+ + 4e \xrightarrow{\text{laccase}} 2H_2O$$

$$E_c^{o'} = 0.93 \text{ V } (vs. \text{ SHE}) \quad (3)$$

here $E_c^{o'}$ was the formal potential at pH 5.0, which was calculated by Nernst equation in the electrolyte solution saturated with O_2 according to the standard potential of O_2/H_2O couple (1.23 V *vs.* SHE).[17] The OCP of the biocathode (E_c^{ocp}) was calculated to be 0.69 V. The measurement of the OCP for biocathode (E_c^{ocp}) was similar to that of E_a^{ocp}, only the glucose in the electrolyte was replaced by the saturated O_2. ABTS was the suitable electron mediator to decrease the over-potential for the reduction of O_2 by laccase in the cathode.[28] Compared to curve a in Fig. 2A, curve b in Fig. 2A showed that once 0.5 mM ABTS was added into the catholyte, the E_c^{ocp} gradually approached to 0.56 ± 0.02 V (n = 3).

In the acidic buffer solution, CV testing showed the $ABTS^{2-}$ could be partly changed to $HABTS^-$ (Fig. S5 in the ESI). The $ABTS^{\bullet-}/HABTS^-$ redox couple is better than $ABTS^{\bullet-}/ABTS^{2-}$ for the reduction of O_2 by laccase because the standard potentials of $ABTS^{\bullet-}/HABTS^-$ and $ABTS^{\bullet-}/ABTS^{2-}$ are 0.57 V and 0.44 V *vs.* SCE, respectively.[29] Interestingly, it was observed that the redox potential of $ABTS^{\bullet-}/HABTS^-$ couple was around 0.55 V (*vs.* SCE) at graphene–AuNPs hybrid electrode (Fig. S5 in the ESI), which was consistent with the measured E_c^{ocp}. This is because the adsorption of the acid media was superior at the surface of AuNPs,[16] more $HABTS^-$ should form at the surface of the electrode, which was more effective for the reduction of O_2 at the electrode surface. UV-vis spectrum (Fig. S6 in the ESI) also demonstrated that $HABTS^-$ was appropriate as the electron mediator for the reduction of O_2 by laccase. The optimal concentration of the ABTS was selected for 0.5 mM, as discussed in Fig. S7 in the ESI, and the performance of ABTS for the reduction of O_2 at the biocathode was shown in Fig. 2B.

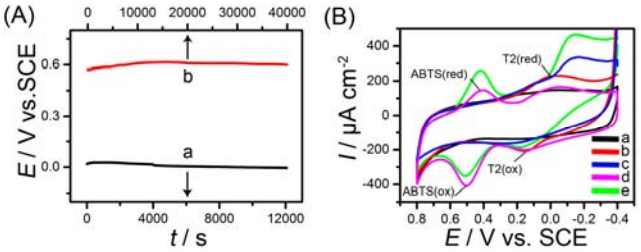

Fig. 2 (A) OCP of the graphene–AuNPs–laccase hybrid electrode in pH 5.0 electrolyte solution saturated with O_2, (a) without ABTS and (b) containing 0.5 mM ABTS. (B) CVs of the graphene–AuNPs electrode (a), graphene–AuNPs–laccase hybrid electrode in pH 5.0 electrolyte solution saturated with N_2 (b) and saturated with O_2 (c), the graphene–AuNPs–laccase hybrid electrode in pH 5.0 electrolyte solution containing 0.5 mM ABTS saturated with N_2 (d) and saturated with O_2 (e). The scan rate was 10 mV s^{-1}.

3.3 The characters of the EBFC.

The EBFC was constructed by the bioanode and biocathode as described. The power density of the EBFC was influenced by the glucose concentration.[30, 31] The results in the EBFC revealed that both of the maximal E_{cell}^{ocv} and P_{max} were obtained when the glucose concentration was 50 mM (Fig. S8 in ESI). The theoretical value of E_{cell}^{ocv} could be calculated to be 1.28 V for the designed EBFC model. The measurement for E_{cell}^{ocv} was shown in Fig. 3A. As expected, the E_{cell}^{ocv} reached to 1.16 ± 0.02 V (n=3, curve a in Fig. 3A). The E_{cell}^{ocv} was improved greatly referring to the reports that were listed in Table 1.

Fig. 3B showed the polarization curve and the power density curve of the EBFC. When the EBFC operated, the output voltage (E_{cell}) in the EBFC could be expressed in terms of the overpotentials associated with different fundamental phenomena as shown the equation: $E_{cell} = E_c^{ocp} - iR_{act,c} - iR_{conc,c} - E_a^{ocp} - iR_{act,a} - iR_{conc,a} - ir_{ohm}$, where the meaning of all the symbols are the same as reference.[32] E_{cell} was affected by the charge transfer derived overpotentials, the concentration overpotentials, and the ohmic overpotentials of the EBFC. Because the EBFC performed generally in the region of the ohmic polarization, the charge transfer derived overpotentials and the concentration overpotentials could be ignored, and E_{cell} could be expressed: $E_{cell} = E_c^{ocp} - E_a^{ocp} - ir_{ohm} = E_{cell}^{ocv} - ir_{ohm}$, which showed a linear relationship between E_{cell} and i in the region of the ohmic polarization. Based on the linear portion of the polarization curve in Fig. 3B ($E_{cell} = -266\ i + 1.03$, $R = 0.997$), the internal resistance of the EBFC (r_{ohm}) was calculated to be about 266 Ω. The power density as a function of the cell current density for the EBFC presented the typical bell-shaped curve[10] as shown curve b in Fig. 3B. Thus, the maximum power output for the EBFC model, P_{max}, was estimated as high as 1.96 ± 0.13 mW cm^{-2} (relative to the geometric area of the Au substrate electrode). Under the optimal conditions and in the absence of glucose or O_2, the blank experimental results showed that the maximal power output of the biofuel cell was only 0.231 ± 0.009 mW cm^{-2} or 0.281 ± 0.008 mW cm^{-2}, respectively; In the absence of glucose oxidase in bioanode or laccase in biocathode, the control experimental results displayed that the maximal power output of the biofuel cell was only 0.447 ± 0.018 mW cm^{-2} or 0.512 ± 0.011 mW cm^{-2}, respectively, which demonstrated that the response was due only to glucose oxidation catalyzed by glucose oxidase and oxygen reduction catalyzed by laccase (in Fig. S9 in

the ESI). When the EBFC reached to the maximum power output, the external load was equal to the r_{ohm}, about 200 Ω, as shown in Fig. 3C. Compared to the P_{max} of the EBFC reported in Table 1, the P_{max} achieved in this work was the highest value in the kind of EBFC.

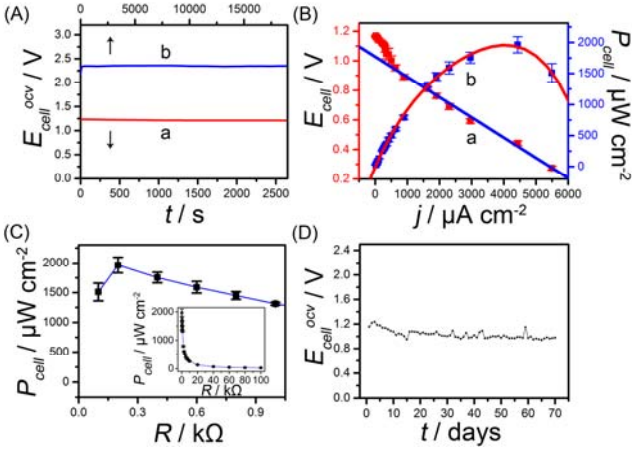

Fig. 3 (A) The E_{cell}^{ocv} of (a) single EBFC unit and (b) two EBFCs units in series. (B) (a) Polarization curve and (b) power density curve of the EBFC, every point was an average value of three independent measurements. (C) Power density of the EBFC *versus* the variable external loads. Inset: the power density *versus* the variable external loads from 100 Ω to 100 kΩ. (D) The relationship between E_{cell}^{ocv} of the EBFC and operation time.

Table 1. Comparison between our EBFC with other EBFCs

P_{max} (μW cm^{-2})	E_{cell}^{ocv} (V)	C (mM)	Electrode material	Ref. No.
1964 ± 130	1.16	50	Graphene–AuNPs hybrid	Present
24.3 ± 4	0.58	100	Graphene	18
1450 ± 240	0.80	400	Carbon fiber sheet	12
740	0.83	15	Carbon nanotube fibers	19
350	0.88	15	Carbon fibers	33
1.36	0.884	1000	Graphite plates	34
1300	0.95	50	Carbon nanotube	10

As the energy device, reasonable lifetime for portable applications[3] and low capacity loss under open circuit conditions[35] are of great importance. EBFCs suffer from a very prominent disadvantage for long-term operation, due to loss in enzyme activity.[18, 34] To test the storage stability of the EBFC, the E_{cell}^{ocv} was continuously measured over 70 days in a quiescent state. Fig. 3D showed that the E_{cell}^{ocv} could reach to 94% of the maximal E_{cell}^{ocv} immediately once the EBFC was assembled. When the E_{cell}^{ocv} was lower than 1 V, the fuels in EBFC were replaced. After 70 days, the E_{cell}^{ocv} of the EBFC still kept 80% of its maximum value. For evaluating the stability of power output for the EBFC, the P_{max} of the EBFC was also tested every day (Fig. S10). After the operation of about 70 days, the P_{max} of EBFC decreased to around 1.30 mW cm^{-2}, which was about 66% of its optimal value. It was reported that the GOD activity deteriorated in the acetic acid buffer solution (pH 5.0) after 4 days,[34] the P_{max} of the EBFC was found to become 50% of its original value after 7 days for graphene electrode.[18] However, the stability of the designed EBFC was improved greatly. It was because AuNPs could provide a suitable microenvironment for enzymes to retain their biological activities. Therefore, the graphene–AuNPs hybrid was a suitable material for the preparation of the EBFC.

The potential value of the EBFC as the power source was also studied. As the curve b in Fig. 3A showed that E_{cell}^{ocv} of the two of the as-prepared EBFC in series could reach to around 2.36 V, the sum of the E_{cell}^{ocv} contributed by two EBFCs, respectively, both the designed EBFC in series could light the red and yellow light-emitting diodes (LEDs) brightly, respectively (Fig. S11 in the ESI).

4. Conclusions

In summary, based on the graphene–AuNPs–GOD bioanode and the graphene–AuNPs–laccase biocathode, a novel EBFC was successfully fabricated. Because of the fast electron transfer from bioanode and biocathode, the constructed EBFC has the high E_{cell}^{ocv} and power output. Both the as-prepared EBFC units in series can light the red and yellow LEDs, and the E_{cell}^{ocv} and P_{max} of the EBFC still retain 80% and 66% of its maximum value after 70 days, respectively. We expect that the proposed strategy can take one step forward for fabricating EBFC in practical application.

Acknowledgements

We gratefully appreciate the National Natural Science Foundation (21175065, 21375059, 21335004 and 21121091), and the National Basic Research Program (2011CB933502) of China.

Notes and references

[a] *State Key Laboratory of Analytical Chemistry for Life Science, School of Chemistry and Chemical Engineering, Nanjing University, Nanjing, 210093, P. R. China. Fax: +86 25 83594976; Tel: +86 25 83686130;* *E-mail: jrzhang@nju.edu.cn; jjzhu@nju.edu.cn.*
[b] *School of Chemistry and Life Science, Nanjing University Jinling college, Nanjing 210089, P. R China.*
† Electronic Supplementary Information (ESI) available. See DOI: 10.1039/b000000x/
‡ These authors contributed equally to this work.

1 M. J. Moehlenbrock and S. D. Minteer, *Chem. Soc. Rev.*, 2008, **37**, 1188.
2 M. J. Cooney, V. Svoboda, C. Lau, G. Martin and S. D. Minteer, *Energy Environ. Sci.*, 2008, **1**, 320.
3 S. C. Barton, J. Gallaway and P. Atanassov, *Chem. Rev.*, 2004, **104**, 4867.
4 X. Y. Yang, G. Tian, N. Jiang and B. L. Su, *Energy Environ. Sci.*, 2012, **5**, 5540.
5 A. Heller, *Phys. Chem. Chem. Phys.*, 2004, **6**, 209.
6 U. Schroder, *Angew. Chem. Int. Edit.*, 2012, **51**, 7370.
7 A. Szczupak, J. Halamek, L. Halamkova, V. Bocharova, L. Alfonta and E. Katz, *Energy Environ. Sci.*, 2012, **5**, 8891.
8 T. Miyake, K. Haneda, N. Nagai, Y. Yatagawa, H. Onami, S. Yoshino, T. Abe and M. Nishizawa, *Energy Environ. Sci.*, 2011, **4**, 5008.
9 I. Willner, *Science*, 2002, **298**, 2407.
10 A. Zebda, C. Gondran, A. Le Goff, M. Holzinger, P. Cinquin and S. Cosnier, *Nat. Commun.*, 2011, **2**, 370.
11 S. Freguia, B. Virdis, F. Harnisch and J. Keller, *Electrochim. Acta*, 2012, **82**, 165.
12 H. Sakai, T. Nakagawa, Y. Tokita, T. Hatazawa, T. Ikeda, S. Tsujimura and K. Kano, *Energy Environ. Sci.*, 2009, **2**, 133.
13 Y. Chen, Y. Li, D. Sun, D. B. Tian, J. R. Zhang and J. J. Zhu, *J. Mater. Chem.*, 2011, **21**, 7604.
14 N. Mano, F. Mao, W. Shin, T. Chen and A. Heller, *Chem. Commun.*, 2003, **4**, 518.

15 X. H. Li, L. Dai, Y. Liu, X. J. Chen, W. Yan, L. P. Jiang and J. J. Zhu, *Adv. Funct. Mater.*, 2009, **19**, 3120.

16 Y. Onal, S. Schimpf and P. Claus, *J. Catal.*, 2004, **223**, 122.

17 D. C. Harris, *Quantitative chemical analysis, 8th ed*, W. H. Freeman and Company, New York, 2010.

18 C. Liu, S. Alwarappan, Z. F. Chen, X. X. Kong and C. Z. Li, *Biosens. Bioelectron.*, 2010, **25**, 1829.

19 F. Gao, L. Viry, M. Maugey, P. Poulin and N. Mano, *Nat. Commun.*, 2010, **1**, 2.

20 J. R. Bard and L. R. Faulkner, *Electrochemical Methods: Fundamentals and Applications, 2nd ed.*, Wiley, New York, 2001.

21 C. S. Shan, H. F. Yang, J. F. Song, D. X. Han, A. Ivaska and L. Niu, *Anal. Chem.*, 2009, **81**, 2378.

22 J. M. Goran, S. M. Mantilla and K. J. Stevenson, *Anal. Chem.*, 2013, **85**, 1571.

23 M. Wooten, S. Karra, M. Zhang and W. Gorski, *Anal. Chem.*, 2014, **86**, 752.

24 Z. Y. Wang, S. N. Liu, P. Wu and C. X. Cai, *Anal. Chem.*, 2009, **81**, 1638.

25 Y. F. Bai, T. B. Xu, J. H. Luong and H. F. Cui, *Anal Chem*, 2014, **86**, 4910.

26 W. Grosse, J. Champavert, S. Gambhir, G. G. Wallace and S. E. Moulton, *Carbon*, 2013, **61**, 467.

27 J. T. Holland, C. Lau, S. Brozik, P. Atanassov and S. Banta, *J. Am. Chem. Soc.*, 2011, **133**, 19262.

28 Y. Liu, M. K. Wang, F. Zhao, B. F. Liu and S. J. Dong, *Chem.-Eur. J.*, 2005, **11**, 4970.

29 S. L. Scott, W. J. Chen, A. Bakac and J. H. Espenson, *J. Phys. Chem.*, 1993, **97**, 6710.

30 N. Mano, *Chem Commun.*, 2008, **19**, 2221.

31 D. Wen, X. L. Xu and S. J. Dong, *Energy Environ. Sci.*, 2011, **4**, 1358.

32 F. Zhao, R. C. T. Slade and J. R. Varcoe, *Chem. Soc. Rev.*, 2009, **38**, 1926.

33 V. Soukharev, N. Mano and A. Heller, *J. Am. Chem. Soc.*, 2004, **126**, 8368.

34 S. Fishilevich, L. Amir, Y. Fridman, A. Aharoni and L. Alfonta, *J. Am. Chem. Soc.*, 2009, **131**, 12052.

35 S. K. Chaudhuri and D. R. Lovley, *Nat. Biotech.*, 2003, **21**, 1229.

Design of the enzymatic biofuel cell with large power output

Yun Chen,[‡a] Panpan Gai,[‡a] Jianrong Zhang,*[a, b] and Jun-Jie Zhu*[a]

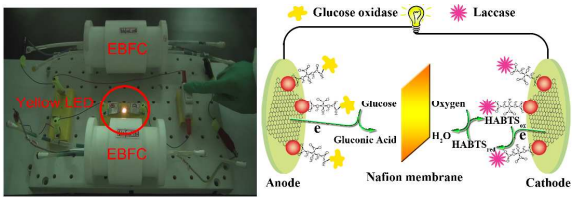

Based on the graphene-AuNPs-GOD bioanode and graphene-AuNPs-laccase biocathode, a novel enzymatic biofuel cell with large power output was successfully designed.